Journal of Geology & Exploration
Vol. 3, No. 1, June 2024 : 13 – 26
E-ISSN 2963-2869

Vulnerability of Mass Movement Zonation Using DEM in Upstream–Kelara Watershed, Jeneponto Regency, Sulawesi Selatan

Fathurrahman*[1], Busthan Azikin[1], A. M. Imran[1]
[1] Geological Engineering Department, Faculty of Engineering, Universitas Hasanuddin, Indonesia
Correspondence e-mail: fathurrahmanhusainmassiara@gmail.com

ABSTRACTS
Mass movement is one of the major natural disasters that claim many lives and property. The Kelara watershed, which is the research area, often encounters land movements that often cause casualties. The problem of mass movement often occurs in the upstream - midstream part of the Kelara watershed with mountainous to hilly morphology with moderately steep to steeply sloping relief. The parameters used in this analysis are lithology, distance from faults, distance from rivers, distance from streets, land use, rainfall, soil type, slope, profile curvature, and slope aspect. The analysis was conducted by giving weights based on the comparison of soil movement events to the class of each parameter using the Weight of Evidence method. Based on the Weight of Evidence method, the mass movement vulnerability zone is divided into five zones, very low vulnerability zone occupies 7.75%, low vulnerability zone occupies 27.11%, medium vulnerability zone occupies 31.76%, high vulnerability zone occupies 21.72%, and very high vulnerability zone occupies 11.66% of the total study area. Based on validation using the AUC value, the Weight of Evidence Method has a value of 0.771 (Fairly Good Model).

ARTICLE INFO
Article History:
Received 14 Feb 2024
Revised 16 Feb 2024
Accepted 05 Jun 2024
Available 30 Jun 2024

Keyword:
Mass Movement Zonation, Weight of Evidence, Kelara Watershed

https://doi.org/10.58227/jge.v3i1.164

INTRODUCTION

Mass Movements (Landslides) are major geological disasters that occur in areas with sloping morphology and high rainfall and can cause loss of life and impact on nature or the environment. Mass movement is a natural event that is currently increasing in frequency (Faruqi et al., 2023; Winahyu et al., 2023). This natural phenomenon turns into a natural disaster when the ground movement causes casualties both in the form of casualties and losses of property and human cultural products. Indonesia, which is partly in the form of hilly and mountainous areas, causes some parts of Indonesia to be prone to mass movement events (Prastowo et al., 2018).

This disaster is closely related to natural conditions such as soil type, rock type, rainfall, land slope, and land cover. In addition, human factors greatly influence the occurrence of landslides, such as forestry land use changes that does not follow the rules and carelessly, logging without selective logging, expansion of settlements in areas with steep topography (Rahmad et al., 2018).

The increase in critical land area, erosion, flooding, sedimentation, and landslides are indicators of the declining carrying capacity of watersheds. Watershed conditions that tend to worsen cause erosion, flooding, sedimentation, and landslides to occur more frequently and tend to increase. One of the most serious problems is landslides (Widianto et al., 2023). These disasters not only cause material losses, but also take a lot of lives. The main cause of landslides is the force of gravity affecting a steep slope, but there are other factors that cause landslides, such as high rainfall, improper land use and geologic structure (Arsyad et al., 2018).

The Kelara watershed, which is the study area, is often found with land movements that often cause casualties. The area where this disaster occurs is the upstream - midstream part of the Kelara watershed with mountainous to hilly morphology. Based on the morphology and data on the occurrence of mass movements sourced from DIBI BNPB, the occurrence of mass movements found in the upstream - midstream of the watershed which generally has a moderately steep - steep relief.

Journal of Geology & Exploration
Vol. 3, No. 1, June 2024 : 13 – 26
E-ISSN 2963-2869

The upstream of the Kelara watershed is in Gowa Regency while the downstream of the Kelara watershed is in Jeneponto Regency with a total area of approximately 39,112 ha covering eight sub-districts namely Bontolempangan, Bongaya, Biringbulu, Tompobulu, Binamu, Kelara, Turatea, and Rumbia. The watershed boundary map used in the study was obtained from the Directorate of Watershed Control Planning and Evaluation (PEPDAS).

One of the stages of landslide disaster mitigation can be mapping or zoning of mass movement vulnerable areas. Mass movement vulnerability zoning can be identified through geographic information system (GIS) easily, quickly, and quite accurately. The mapping is done by mapping the factors that cause the occurrence of mass movement in the area by giving a value to each parameter that causes it, so that the mass movement vulnerability zone is obtained. Giving value or weighting in this research is based on field survey data and spatial data, especially DEM (Digital Elevation Model). Considering the availability of easily accessible spatial data, various data for parameters can be collected for this analysis (Bakri et al., 2021; Thamsi et al., 2021).

Administratively, the research location of ground motion susceptibility zoning is located in Gowa Regency and Jeneponto Regency of South Sulawesi Province. Astronomically it is located at 119° 44' 19.85“ East - 119° 56' 15.93” East (East Longitude) and 05° 19' 28.94” South - 05° 36' 35.19” South (South latitude).

The purpose of this research is to map the mass movement vulnerability zone using DEM in the Upstream-Midstream part of Kelara Watershed, Gowa Regency and Jeneponto Regency, South Sulawesi Province. The ovjectives of this research is to know the class and value of the mass movement vulnerability zone of each parameter used, to know the effect of each parameter on mass movement, to know the mass motion vulnerability zone in the research area.

METHODS

The research was conducted using a combination of field survey data and spatial data. mass movements event data was sourced from field surveys, BNPB inventory, and satellite image identification. Parameter data was sourced from various spatial data providers. The main source of parameter data is DEM (Digital Elevation Model). The DEM data used is Alos Palsar DEM which has a resolution of 12.5 meters, this DEM data is better when compared to DEMNAS data which only has a resolution of 30 meters. Each parameter used is processed using ArcGis software and presented as a thematic map of mass movement parameters.

Table 1. Research Data and Sources

No	Data	Sources
1	Mass Movements event	Field Survey, BNPB, and satellite image identification
2	Watershed Boundary	Directorate of Watershed Control Planning and Evaluation (PEPDAS)
3	Lithology	Field survey and Regional Geologic Map Ujungpandang, Benteng, dan Sinjai Sheet
4	Geologic Structure	Field survey and Regional Geologic Map Ujungpandang, Benteng, dan Sinjai Sheet
5	River	Indo Geospasial
6	Street	Open Street Map
7	Land Use	WebGIS Ministry of Environtment and Forestry
8	Soil	FAO UNESCO
9	Rainfall	CHIRPS: Rainfall Estimates from Rain Gauge and Satellite Observations
10	Slope	Alos Palsar DEM
11	Profile Curvature	Alos Palsar DEM
12	Slope Aspect	Alos Palsar DEM

The method used in this mass movement vulnerability zoning is Weight of Evidence (WoE). Weighting is done on each parameter map that has been made in the previous stage. This weighting is the result of calculations using the WoE method based on the comparison of mass movement events

Journal of Geology & Exploration
Vol. 3, No. 1, June 2024 : 13 – 26
E-ISSN 2963-2869

to the class of each parameter. The WoE model is a data-driven quantitative technique, using a number of data combinations to produce maps from weighted data, both continuous and categorical, based on prior and posterior probabilities (Pamela et al., 2018; Thamsi et al., 2019)
WoE's formulation is as follows:

$$W^{+} = ln\left[\frac{P\{N_j|S\}}{P\{N_j|\bar{S}\}}\right] = ln\left(\frac{\frac{P(N_j \cap S)}{P(S)}}{\frac{P(N_j \cap \bar{S})}{P(\bar{S})}}\right) = ln\left(\frac{\frac{Npix\ landslide\ in\ class}{Npix\ total\ landslide\ area}}{\frac{Npix\ stable\ area\ in\ class}{Npix\ total\ stable\ area}}\right)$$

$$W^{-} = ln\left[\frac{P\{\bar{N}_j|S\}}{P\{\bar{N}_j|\bar{S}\}}\right] = ln\left(\frac{\frac{P(\bar{N}_j \cap S)}{P(S)}}{\frac{P(\bar{N}_j \cap \bar{S})}{P(\bar{S})}}\right) = ln\left(\frac{\frac{Npix\ landslide\ outside\ class}{Npix\ total\ landslide\ area}}{\frac{Npix\ stable\ area\ outside\ class}{Npix\ total\ stable\ area}}\right)$$

$$Weight = W^{+} - W^{-}$$

where W+ is the weighted probability of mass movements in a geofactor class (positive weight). W- is the weighted improbability of ground motion in a geofactor class (negative weight). Nj is the number of pixels in geofactor class J. S is the total number of pixels containing mass movements in the whole area, and P is the probability value.

Validation of the mass movement vulnerability map was conducted to determine the accuracy of the model. The accuracy of the model using the AUC-ROC method. The AUC (Area Under Curve) value is an index value formed from a comparison graph between the percentage of the total area of the parameter class area causing mass movements and the percentage of the total number of mass movements. (Pamela et al., 2018)

Table 2. AUC Values

AUC Values	Description
0,9	Very Good Model
0,8 – 0,9	Good Model
0,7 – 0,8	Medium / Fair Model
<0,6	Poor Model

RESULTS AND DISCUSSION

Mass Movement Event

Mass movement event data identification of satellite imagery was carried out using Google satellite by creating polygons based on the appearance of mass movement seen in satellite imagery. Data on mass movement events sourced from BNPB DIBI inventory collected by adjusting mass movement events to the research location, data collected in the form of coordinate points, time, and other documentation.

Figure 1. Mass Movements in Field Survey, Mass Movement from DIBI BNPB, Mass Movement from satellite imagery identification

Journal of Geology & Exploration
Vol. 3, No. 1, June 2024 : 13 – 26
E-ISSN 2963-2869

Data on mass movement events at the research site were collected from various sources, such as visual identification through satellite imagery as much as 31 data, identification from field observations as much as 5 data, and inventory of mass movement events as much as 5 data from the Indonesian Disaster Information Data (DIBI) of BNPB. All of these data will be used for mass movement analysis and 30% of random data will be used for ROC-AUC validation.

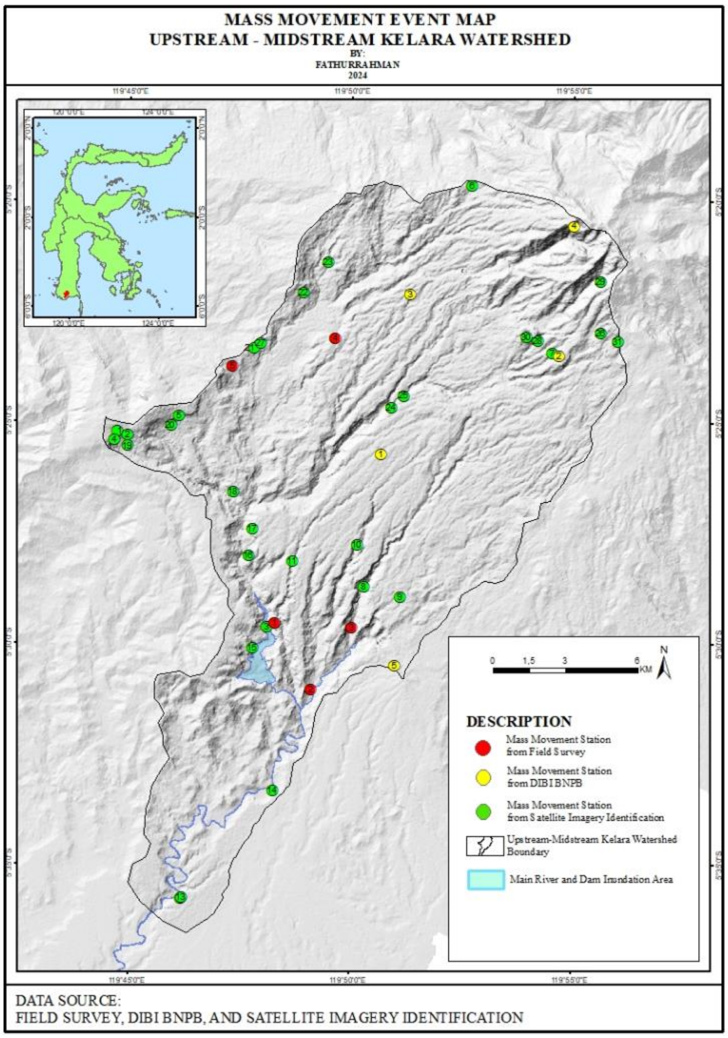

Figure 2. Mass Movement Event Map Upstream - Midstream Kelara Watershed

Lithology Parameter

Lithological data was obtained from the Regional Geological Map of Ujungpandang, Benteng and Sinjai Sheet mapped by Sukamto and Supriatna (1982) and field survey mapped by the author in Bossolo area.

Lithological parameters can be composed of rocks or soils that are the result of the weathering of these rocks. Lithology is an important factor in the occurrence of mass movement. Lithologies with a high level of resistance are less likely to experience mass movement. While lithologies with low resistance such as soil have more potential for mass movement to occur (Prastowo et al., 2018).

The research showed that mass movement occurred in Qlv (Lompobatang Volcano Rocks) with a percentage of 63.8%, Qlvb (Breccia Member of Lompobatang Volcano Rocks) 3.6%, Qlvp1 (Parasitic Eruption of Lompobatang Volcano Rocks) 4.6%, Tmc (Camba Formation) 4.6%, Tpbv (Baturape-Cindako Volcano Rocks) 23.4%, and no mass movement was found in Qac (Alluvium and Coastal Deposits).

Journal of Geology & Exploration
Vol. 3, No. 1, June 2024 : 13 – 26
E-ISSN 2963-2869

Distance from Fault Parameter

The fault zones used were obtained from the Regional Geological Map of Ujungpandang, Benteng, and Sinjai Sheet mapped by Sukamto and Supriatna (1982) and field surveys mapped by the author in the Bossolo area.

Generally, faults are formed as joints that cause cracks in the lithology. The fault zone becomes an unstable area and has the potential for landslides, especially around areas with high slopes (Anwar et al., 2023; Eden et al., 2020; Thamsi et al., 2023).

The study showed that mass movement occurred at distances (0 - 100) meters with a percentage of 1.3%, distances (200 - 500) meters as much as 9.1%, distances (500 - 1000) meters as much as 11.6%, distances >1000 meters as much as 78.1%, and no mass movement was found at a distance of (100 - 200) meters.

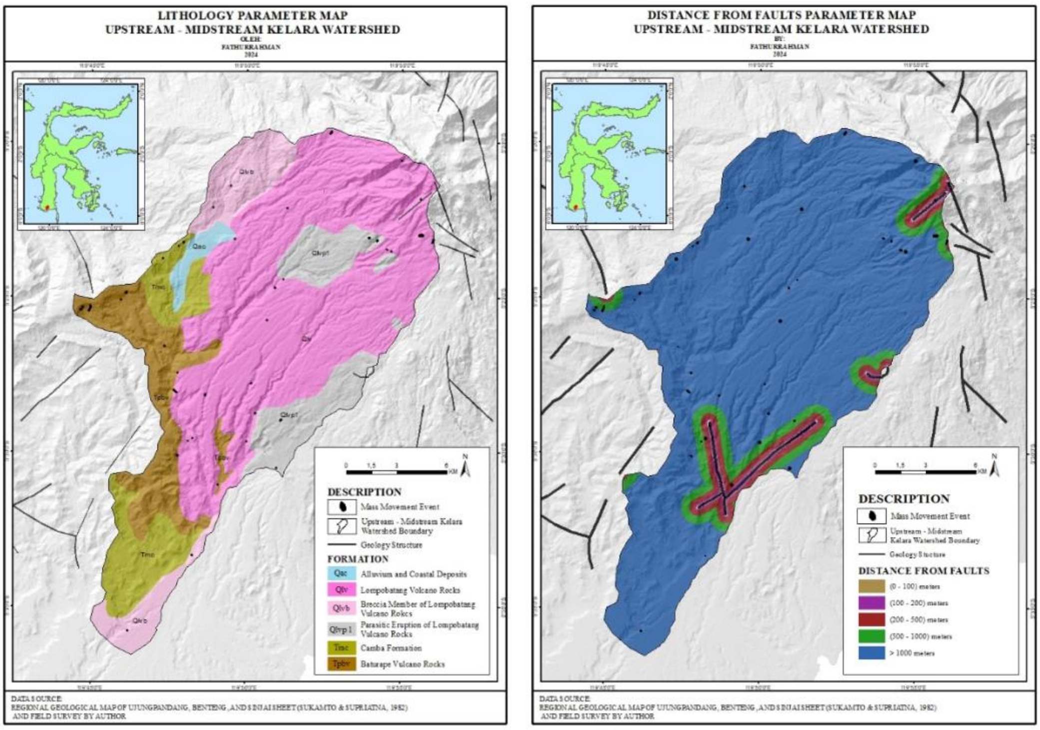

Figure 3. Lithology Parameter Map and Distances from Faults Parameter Map

Distances from River Parameter

River data was obtained from the Rupa Bumi Indonesia (RBI) map from Ina-Geospasial published by the Geospatial Information Agency.

It is the distance from the river that is most likely to control the potential for landslides to occur where the banks of the river wall are likely to fall due to erosion from the river flow or from the slope of the surrounding area (Eden et al., 2020).

Mass movement occurred at a distance of (0 - 50) meters as much as 26.5%, at a distance of (50 - 100) meters as much as 12.4%, at a distance of (100 - 200) meters as much as 21.3%, and at a distance of >200 meters as much as 39.8%.

Distances from Street Parameter

Streets polyline spatial data was obtained from OSM MAP (Open Street Map) which is updated regularly.

Distance from the street can cause mass movement, this is caused by vehicle traffic around the slope. Mass movement does not occur immediately but through a process in the form of roads traveled by vehicles experiencing cracks which, if left unchecked, will eventually lead to landslides (Hidayah et al., 2017).

Mass movement was found at a distance of (0 - 50) meters as much as 1.3%, a distance of (50 -100) meters as much as 1.3%, a distance of (100 - 200) meters as much as 7.8%, and a distance of >200 meters as much as 89.7%.

Journal of Geology & Exploration
Vol. 3, No. 1, June 2024 : 13 – 26
E-ISSN 2963-2869

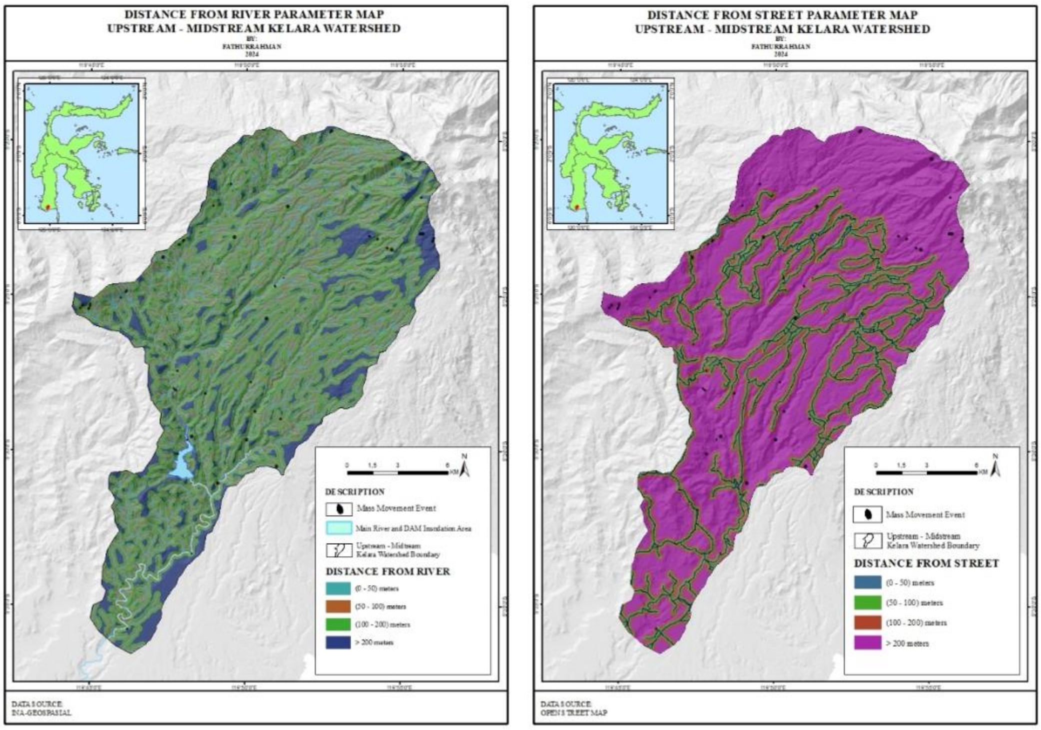

Figure 4. Distances from River Parameter Map and Distances from Streets Parameter Map

Land Use Parameter

Land use information was obtained from the 2019 Land Cover Map from the Ministry of Environment and Forestry webgis.

Raditya & Setiawan (2018) explained that the type of land use that determines the level of potential landslide hazard (prone to very prone) is moorland, settlements, shrubs, rice fields, and fields. Land that loses its land cover vegetation will become cracked during the dry season and during the rainy season, water will easily seep into the soil through the cracks so that it can cause the soil layer to become water-saturated and then increase the risk of mass movement.

Mass movement in scrub areas was 2.5%, secondary dryland forest areas were 48%, dryland agricultural areas were 0.6%, mixed dryland agriculture was 40.4%, open land was 8.5%, and no mass movement was found in primary dryland forest, plantation forest, and settlement areas.

Rainfall Parameter

Rainfall data was obtained from CHIRPS: Rainfall Estimates from Rain Gauge and Satellite.

The scoring is based on the size of the average annual rainfall in millimeters. The higher the rainfall in an area, the higher the likelihood of ground motion, and the lower the rainfall in an area, the lower the risk of mass movement. (Raditya & Setiawan, 2018).

The map used is the processing of rainfall data for 2013-2022 with a value of 2160.32-3297.25 mm. Mass movement is found in the medium zone (2000 - 3000mm) as much as 53.5% and in the wet zone (3000 - 4000 mm) as much as 46.5%.

Journal of Geology & Exploration
Vol. 3, No. 1, June 2024 : 13 – 26
E-ISSN 2963-2869

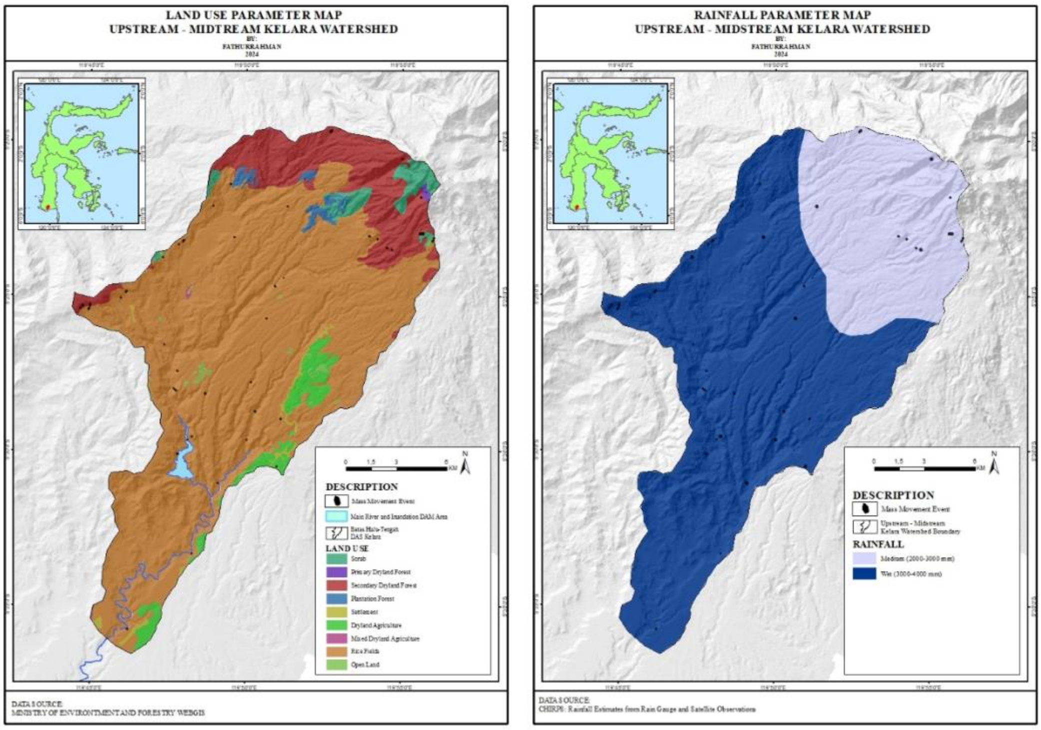

Figure 5. Land Use Parameter Map and Rainfall Parameter Map

Soil Type Parameter

Soil type data was obtained from the FAO-UNESCO Digital Soil Map of the World. The data is in the form of polygons that show differences in soil types.

Soil texture can determine the water system in the soil, in the form of the ability to pass water, penetration, infiltration rate, and the ability to bind water by the soil (Hidayah et al., 2017). Soil texture can be determined by the content of clay, silt and sand based on the USDA classification.

Table 3. Soil texture and composition based on USDA soil texture classification

Soil Name	Texture	Clay%	Silt%	Sand%
Chromic Luvisol	Clay – Loam	35	30	35
Eutric Cambisol	Loam	21	37	42
Humic Cambisols	Loam	17	42	41
Dystric Nitosols	Clay	54	25	21
Pellic Vertisols	Clay	51	26	21

The percentage of mass movement occurrence in the research area is Chromic Luvisols (Clay-Loam) as much as 3.6%, Dystric Nitosols (Loam) as much as 38.9%, Eutric Cambisols (Loam) as much as 18.1%, Humic Cambisols (Clay) as much as 39.4%, and not found in Pellic Vertisols (Clay).

Slope Parameter

The slope was obtained from Alos Palsar DEM processing using the Van Zuidam classification. The slope parameter, is the level of slope reflected in the morphology of the slope. The greater the level of slope will generally increase the possibility of mass movement in an area. This is also related to the gravitational force that pulls the rock mass from top to bottom. The higher the slope, the easier it is for rocks to be pulled downward, resulting in mass movement (Prastowo et al., 2018).

Mass movement on slope (0 - 2)º as much as 0.6%, slope (2 - 5)º as much as 3.6%, slope (5 - 8)º as much as 2.6%, slope (8 - 12)º as much as 4.1%, slope (12 - 29)º as much as 54%, slope (29 - 55)º as much as 33.8%, slope >55º as much as 1.3%.

Journal of Geology & Exploration
Vol. 3, No. 1, June 2024 : 13 – 26
E-ISSN 2963-2869

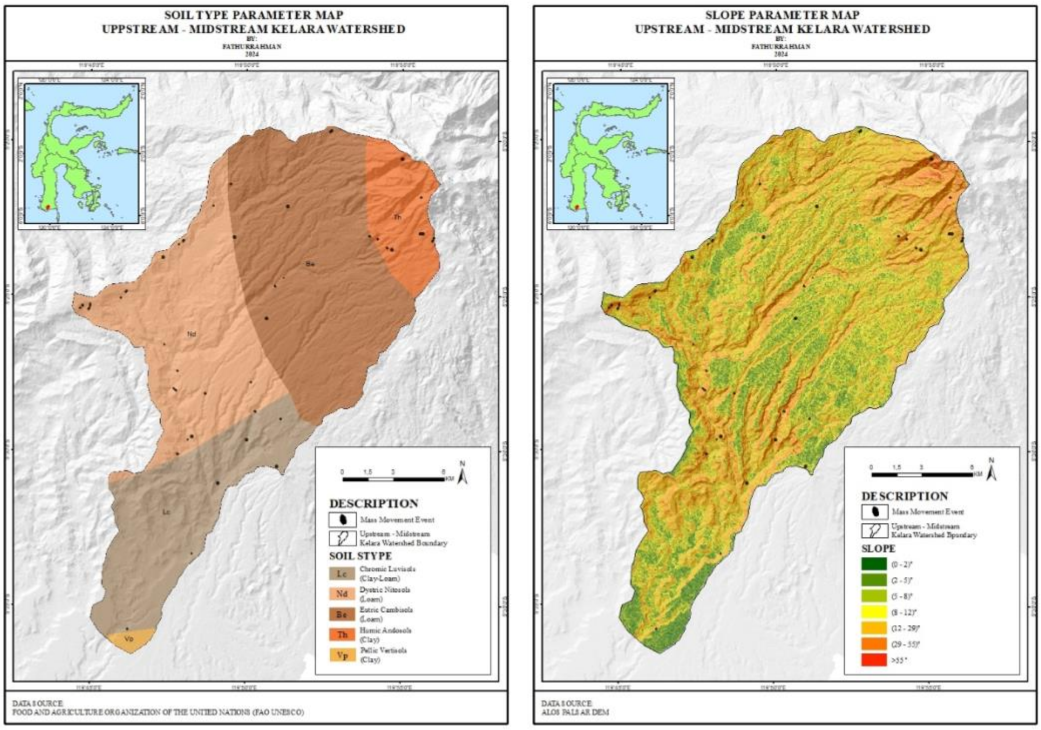

Figura 6. Soil Type Parameter Map and Slope parameter Map

Profile CurvatureParameter

The profile curvature is obtained from the processing of the Alos Palsar DEM. In this case, the curvature profile polygon is divided into concave and convex.

The passage time of surface water also affects the stability of the soil or ground. Concave slopes can hold more water and retain it longer than convex slopes. As a result, the concave slope profile of the area has a higher probability of landslides than convex areas. (Eden et al., 2020).

Mass movement in this study on concave slope profiles was 48.8% and convex was 51.2%.

Slope Aspect Parameter

Slope aspect is obtained from Alos Palsar DEM processing. The aspect parameter is a different parameter in each study area. Therefore, it has been interpreted that it should be examined together with other parameters rather than being an effective parameter in terms of landslide susceptibility alone. Aspect parameters are generally closely related to climatic conditions. They determine the influence of rain direction, amount of sunshine, solar heat, soil moisture, wind and air dryness (Cellek, 2022).

Mass movement in the north direction was 3.2%, northeast was 0.6%, east was 4.3%, southeast was 18.4%, south was 20.1%, southwest was 17.3%, west was 24.4%, northwest was 11.6% and no mass movement were found in flat areas.

Journal of Geology & Exploration
Vol. 3, No. 1, June 2024 : 13 – 26
E-ISSN 2963-2869

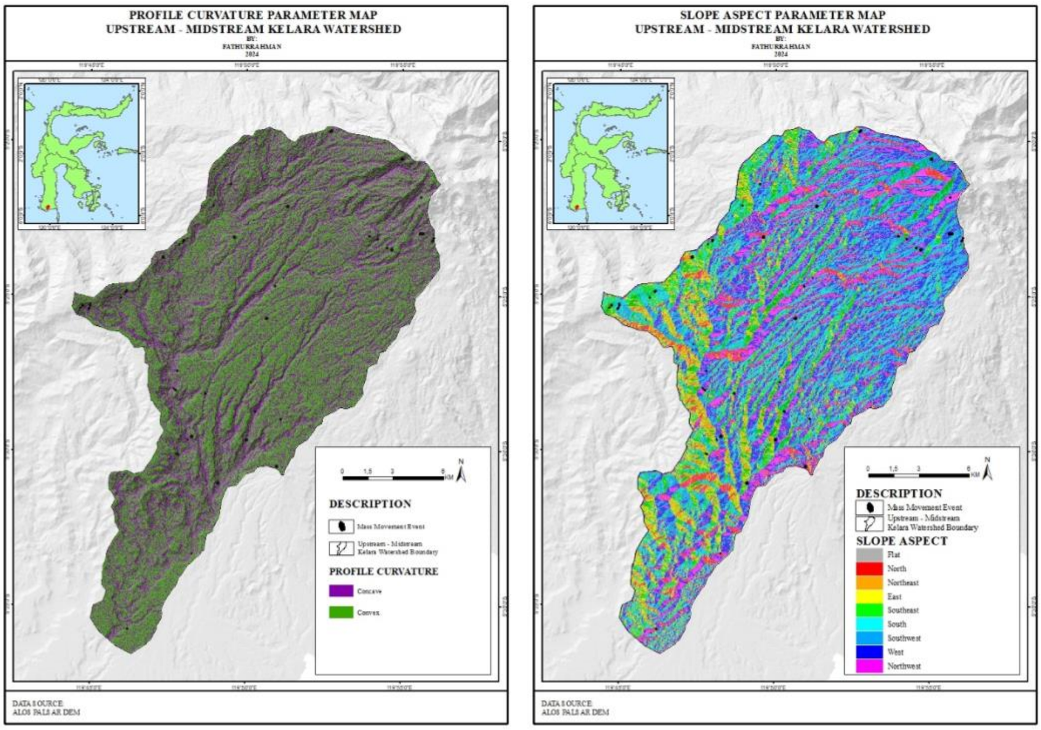

Figure 7. Profile Curvature Parameter Map and Slope Aspect Parameter Map

Mass Movement Vulnerability Zonation

Mass movement vulnerability zoning is done by comparing the occurrence of land movement in the study area with related parameters, then calculating with the Weight of Evidence method.

Based on calculations using the Weight of Evidence method for all classes of each parameter, the following results are obtained:

Table 4. Calculation of the weight of each parameter class using the WoE Method

Parameter	**Class**	**Npix landslide inside class**	**Npix landslide outside class**	**Npix stable area inside class**	**Npix stable area outside class**	**w+**	**W-**	**Weight**
Lithology	Qac	0	475	38814	2069778	-	0,019	-
	Qlv	303	172	1105172	1003420	0,196	-0,273	0,470
	Qlvb	17	458	252939	1855653	-1,209	0,091	-1,301
	Qlvp 1	22	453	189468	1919124	-0,663	0,047	-0,709
	Tmc	22	453	221126	1887466	-0,817	0,063	-0,881
	Tpbv	111	364	301073	1807519	0,493	-0,112	0,605
		475		2108592				
Distance from Faults	(0 – 100) meters	6	469	24222	2084370	0,095	-0,001	0,096
	(100 – 200) meters	0	475	25164	2083428	-	0,012	-
	(200 – 500) meters	43	432	79120	2029472	0,881	-0,057	0,937
	(500 – 1000) meters	55	420	146315	1962277	0,512	-0,051	0,563
	> 1000 meters	371	104	1833771	274821	-0,107	0,519	-0,626
		475		2108592				

Journal of Geology & Exploration
Vol. 3, No. 1, June 2024 : 13 – 26
E-ISSN 2963-2869

Table 4. Calculation of the weight of each parameter class using the WoE Method (Continued)

Parameter	Class	Npix landslide inside class	Npix landslide outside class	Npix stable area inside class	Npix stable area outside class	w+	W-	Weight
Distance from River	(0 – 50) meters	126	349	595873	1512719	-0,063	0,024	-0,087
	(50 – 100) meters	59	416	535215	1573377	-0,715	0,160	-0,875
	(100 – 200) meters	101	374	647733	1460859	-0,370	0,128	-0,496
	> 200 meters	189	286	329771	1778821	0,934	-0,337	1,271
		475		2108592				
Distance from Street	(0 – 50) meters	6	469	219205	1889387	-2,108	0,097	-2,205
	(50 – 100) meters	6	469	195056	1913536	-1,991	0,084	-2,075
	(100 – 200) meters	37	438	325991	1782601	-0,685	0,087	-0,772
	> 200 meters	426	49	1368340	740252	0,323	-1,225	1,548
		475		2108592				
Land Use	Scrub	12	461	52526	2047423	0,01417	0,000	0,015
	Primary Dryland Forest	0	2273	2273	2097676	-	1,571	-
	Secondary Dryland Forest	227	246	290210	1809739	1,24492	-0,505	1,750
	Plantation Forest	0	23183	23183	2076766	-	3,903	-
	Settlement	0	19582	19582	2080367	-	3,733	-
	Dryland Agriculture	3	470	74256	2025693	-1,71833	0,030	-1,748
	Mixed Dryland Agriculture	191	282	1418606	681343	-0,51458	0,608	-1,123
	Rice Field	0	211327	211327	1888622	-	6,208	-
	Open Land	40	433	7986	2091963	3,10176	-0,085	3,186
		473		2099949				
Rainfall	Medium (2000 - 3000 mm)	254	221	625191	1478201	0,58727	-0,412	1,000
	Wet (3000 - 4000 mm)	221	254	1478201	625191	-0,41243	0,587	-1,000
		475		2103392				

Journal of Geology & Exploration
Vol. 3, No. 1, June 2024 : 13 – 26
E-ISSN 2963-2869

Soil Type	Chromic Luvisols	17	458	460733	1647859	-1,80914	0,210	-2,019
	Dystric Nitosols	185	290	607603	1500989	0,30130	-0,154	0,455
	Eutric Cambisols	86	389	836168	1272424	-0,78402	0,305	-1,089
	Humic Cambisols	187	288	188193	1920399	1,48410	-0,407	1,891
	Pellic Vertisols	0	15895	15895	2092697	-	3,518	-
		475		2108592				

Table 4. Calculation of the weight of each parameter class using the WoE Method (Continued)

Parameter	**Class**	**Npix landslide inside class**	**Npix landslide outside class**	**Npix stable area inside class**	**Npix stable area outside class**	**w+**	**W-**	**Weight**
Slope	(0 – 2) %	3	40730	40730	2061206	-1,104	4,488	-5,592
	(3 – 7) %	17	450	190917	1911019	-0,914	0,058	-0,972
	(8 – 13) %	12	455	385248	1716688	-1,964	0,176	-2,141
	(14 – 20) %	19	448	375089	1726847	-1,478	0,155	-1,633
	(21 – 55) %	252	215	890097	1211839	0,242	-0,225	0,467
	(56 – 140) %	158	309	215549	1886387	1,194	-0,305	1,498
	> 140 %	6	461	4306	2097630	1,836	-0,011	1,847
		467		2101936				
Profile Curvature	*Concave*	243	232	895477	1212240	0,186	-0,163	0,349
	Convex	232	243	1212240	895477	-0,163	0,186	-0,349
		475		2107717				
Slope Aspect	Flat	0	0	0	2101728	-	-	-
	North	15	452	127307	1974421	-0,634	0,030	-0,664
	Northeast	3	464	89974	2011754	-1,897	0,037	-1,934
	East	20	447	156423	1945305	-0,553	0,034	-0,586
	Southeast	86	381	304899	1796829	0,239	-0,047	0,285
	South	94	373	365366	1736362	0,147	-0,034	0,180
	Southwest	81	386	382077	1719651	-0,047	0,010	-0,057
	West	114	353	377239	1724489	0,307	-0,082	0,390

Journal of Geology & Exploration
Vol. 3, No. 1, June 2024 : 13 – 26
E-ISSN 2963-2869

Northwest	54	413	298443	1803285	-0,205	0,030	-0,236
	467		2101728				

Reclassification is performed on each parameter based on the calculations from both methods to obtain a map of mass movement vulnerability zones. This zoning is divided into five zones, very low vulnerability zone, low vulnerability zone, medium vulnerability zone, high vulnerability zone, and very high vulnerability zone.

Based on validation using the AUC value, the Weight of Evidence method has a value of 0.771. Based on the Weight of Evidence method, the mass movement vulnerability zone is divided into five zones, very low vulnerability zone occupies 7.75%, low vulnerability zone occupies 27.11%, medium vulnerability zone occupies 31.76%, high vulnerability zone occupies 21.66%, and very high vulnerability zone occupies 11.66% of the total study area.

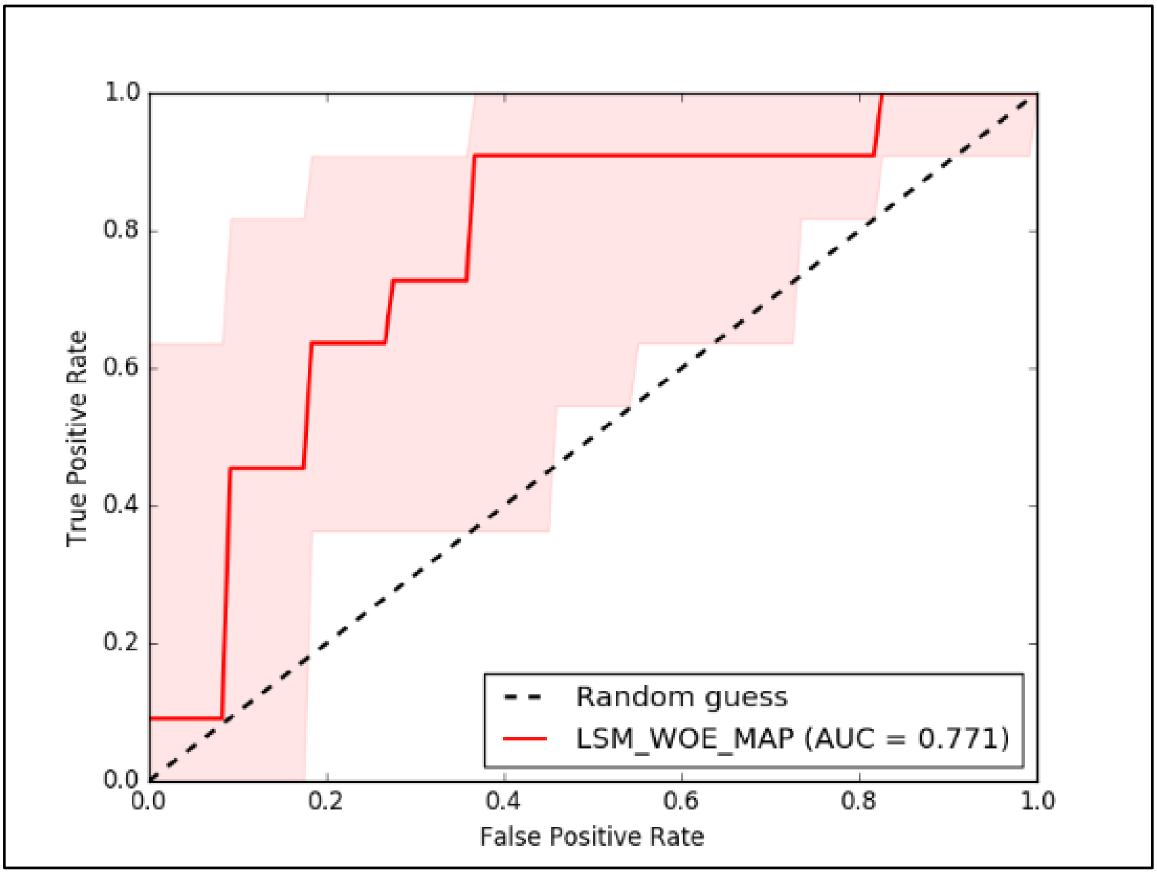

Figure 8. AUC (Area Under Curve) value chart

Journal of Geology & Exploration
Vol. 3, No. 1, June 2024 : 13 – 26
E-ISSN 2963-2869

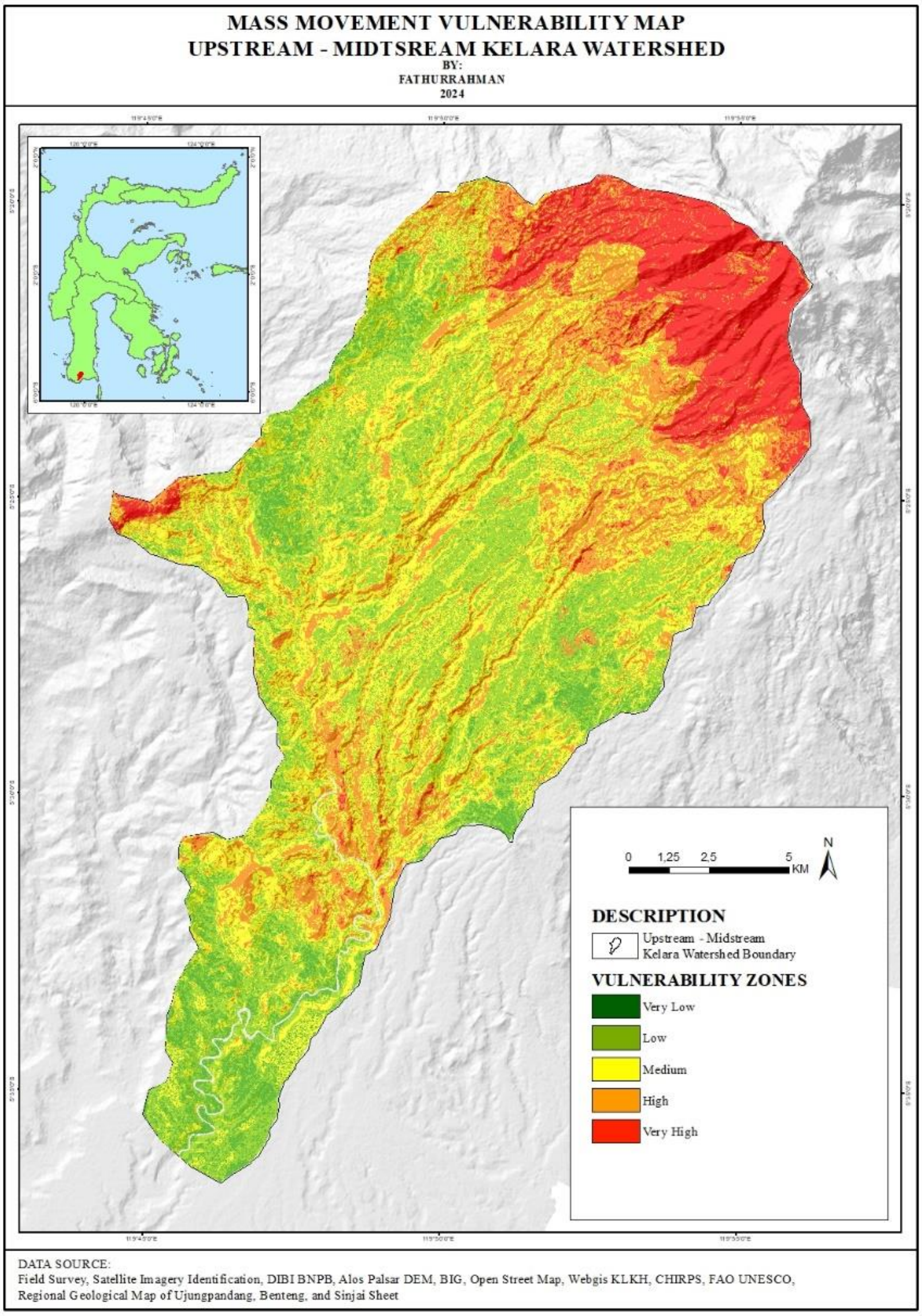

Figure 9. Mass Movement Vulnerability Map of Upstream - Midstream Kelara Watershed

CONCLUSION

Mass movement vulnerability zonation of the upstream-midstream Kelara watershed was conducted using Weight of Evidence on mass movement events and eleven different parameters. Based on the modeling conducted, the mass mobement vulnerability zone is divided into five zones, very low vulnerability zone occupies 7.75%, low vulnerability zone occupies 27.11%, medium vulnerability zone occupies 31.76%, high vulnerability zone occupies 21.72%, and very high vulnerability zone occupies 11.66% of the total study area. Based on validation using the AUC value, the Weight of Evidence Method has a value of 0.771 (Fairly Good Model).

ACKNOWLEDGMENT

The author would like to thank the related parties who have provided support for this research.

Journal of Geology & Exploration
Vol. 3, No. 1, June 2024 : 13 – 26
E-ISSN 2963-2869

REFERENCE

Anwar, H., Mahendra, R. E., Bakri, H., Thamsi, A. B., & ... (2023). Rancangan Penambangan Jangka Pendek Pada Pit Utara di PT Tubindo Kabupaten Bulungan Provinsi Kalimantan Utara. *Jurnal …*. https://jurnal.fti.umi.ac.id/index.php/JG/article/view/142

Arsyad, U., Barke y, R., & Matandung, K. K. (2018). Karakteristik Tanah Longsor di Daerah Aliran Sungai Tangka. *Jurnal Hutan Dan Masyarakat*, *10*(1), 203–214.

Bakri, H., Harwan, H., Thamsi, A. B., Nur, I., & ... (2021). Paragenesis Prospek Endapan Bijih Besi Daerah Tanjung Kecamatan Bontocani Kabupaten Bone, Sulawesi Selatan. *Jurnal …*. https://jurnal.teknologiindustriumi.ac.id/index.php/JG/article/view/971

Cellek, S. (2022). The Effect of Aspect on Landslide and Its Relationship with Other Parameters. In *Landslides*. IntechOpen. https://doi.org/10.5772/intechopen.99389

Eden, J. T., Alimuddin, I., & Azikin, B. (2020). Modeling vulnerability density of landslide using IFSAR DEM in Manuju and Bungaya District Gowa Regency, South Sulawesi. *IOP Conference Series: Earth and Environmental Science*, *500*(1). https://doi.org/10.1088/1755-1315/500/1/012048

Faruqi, M. F. Al, Yusuf, F. N., Anwar, H., & Thamsi, A. B. (2023). Reclamation Plan on Stone Land of The Ex-Nickel Mining at PT Vale Indonesia Tbk Central Pinnacle Condemnation. *Journal of Geology and Exploration*, *2*(1), 13–23. https://doi.org/10.58227/JGE.V2I1.46

Hidayah, A., Paharuddin, & Massinai, Muh. A. (2017). ANALISIS RAWAN BENCANA LONGSOR MENGGUNAKAN METODE AHP (ANALIYTICAL HIERARCHY PROCESS) DI KABUPATEN TORAJA UTARA. *Jurnal Geocelebes*, *1*(1), 1–4.

Pamela, Sadisun, I. A., Kartiko, R. D., & Arifianti, Y. (2018). Metode Kombinasi Weight of Evidence (WoE) dan Logistic Regression (LR) untuk Pemetaan Kerentanan Gerakan Tanah di Takengon, Aceh. *Jurnal Lingkungan Dan Bencana Geologi*, *9*(2), 77–86.

Prastowo, R., Trianda, O., & Novitasari, S. (2018). Identifikasi Kerentanan Gerakan Tanah Berdasarkan Data Geologi Daerah Kalirejo, Kecamatan Kokap, Kabupaten Kulonprogo, Yogyakarta. *KURVATEK*, *3*(2), 31–40.

Raditya, F. T., & Setiawan, B. H. (2018). Analisis Spasial Kawasan Rawan Longsor di Kecamatan Pangentan Kabupaten Banjarnegara. *Media Agrosains*, *4*(1), 30–40.

Rahmad, R., Suib, S., & Nurman, A. (2018). Aplikasi SIG Untuk Pemetaan Tingkat Ancaman Longsor Di Kecamatan Sibolangit, Kabupaten Deli Serdang, Sumatera Utara. *Majalah Geografi Indonesia*, *32*(1), 1. https://doi.org/10.22146/mgi.31882

Sukamto, R., & Supriatna, S. (1982). *Geologi Lembar Ujungpandang, Benteng, dan Sinjai Skala 1:250.000*. Pusat Penelitian dan Pengembangan Geologi Direktorat Pertambangan Umum Departemen Pertambangan dan Energi.

Thamsi, A. B., Anwar, H., Bakri, S., Harwan, H., & Juradi, M. I. (2019). Penerapan Sistem Informasi Geografis Untuk Mengidentifikasi Tingkat Bahaya Longsor Di Kec. Sabbang, Kab. Luwu Utara,Prov. Sulawesi Selatan. *Jurnal Geomine*, *7*(1), 45–55. https://doi.org/10.33536/jg.v7i1.340

Thamsi, A. B., Bakri, H., Harwan, H., & ... (2021). Karakteristik Mineralogi Bijih Besi Daerah Kadong-Kadong, Kabupaten Luwu, Provinsi Sulawesi Selatan. *Jurnal …*. http://ejournal.ft.unsri.ac.id/index.php/JP/article/download/454/601

Thamsi, A. B., Yusuf, F. N., Rahma, K., & Wakila, M. H. (2023). Analisis Perbandingan Pencampuran Bijih Nikel High Grade Limonit Dan Low Grade Saprolit Untuk Memenuhi Permintaan Pasar Pada PT Mandiri Mineral Perkasa. *JNANALOKA*. https://www.lenteradua.net/jurnal/index.php/jnanaloka/article/view/113

Widianto, A., Husain, J. R., & Yusuf, F. N. (2023). Groundwater Quality Analysis In Sidomulyo Hamlet, Argomulyo Village, Kalaena District East Luwu County. *Journal of Geology and Exploration*, *2*(1), 32–41. https://doi.org/10.58227/JGE.V2I1.51

Winahyu, P. S., Sugiarto, A. Z. P., Tabitha, T., Haerudin, N., & Mulyasari, R. (2023). Flood Management Strategy Based on Community Perception in Rajabasa Area, Bandar Lampung City. *Journal of Geology and Exploration*, *2*(1), 8–12. https://doi.org/10.58227/JGE.V2I1.44